Electromigration Analyses of Open TSVs

W. H. Zisser*†,H. Ceric*†,R. L. de Orio*, and S. Selberherr*
*Institute for Microelectronics, TU Wien, Gußhausstraße 27-29/E360, A-1040 Wien, Austria
†Christian Doppler Laboratory for Reliability Issues in Microelectronics
Email: {zisser|ceric|orio|selberherr}@iue.tuwien.ac.at

***Abstract*—A study of electromigration in open through silicon vias (TSVs) is presented. First, the possible effects of the aluminium/tungsten interface are studied in a very simplified structure to find the parameters utmost concerning electromigration. The blocking interface without vacancy sink is found to have the highest resulting vacancy concentrations. This result is further used to model the interface inside the cylindric TSV structure. The simulations show that the highest stresses are located at the inner surface of the aluminium cylinder above the interface between aluminium and tungsten. This is near the region where the current is introduced into the TSV, which happens to be the location of the highest current density at the interface.**

I. Introduction

Three-dimensional (3D) integration is a promising approach for the development of systems with higher performance and increased densities in smaller circuit board areas. Interconnections for 3D integration circuits, though, include components not used in planar 2D architectures, such as through silicon vias (TSVs) and solder bumps. The reliability of these structures is crucial for the reliability of 3D integrated circuits (3D-ICs). Although a lot of investigations regarding the reliability of these interconnects are performed, still there is lack of knowledge about the mechanisms responsible for their failure.

Open through silicon vias introduced in [1] are a TSV concept in which the cylindric structure is coated, rather than entirely filled with the conducting metal. The advantage of this technology, is that it can reduce the stress originating from the mismatched thermal expansion coefficients between the substrate and the TSV. In this work we investigate the possible electromigration (EM) reliability issues associated with this particular TSV technology.

The paper is organized as follows. Section II describes the geometry under consideration and the approach followed in order to model electromigration in such structures. In Section III the results are presented and the main findings are discussed. Section IV summarises and concludes the work.

II. Approach

The TSV geometry considered is shown in Fig. 1. Here, the tungsten, shown in red, forms an empty cylinder closed on the bottom side. Below that (not shown in figure) an aluminium plate is placed on which a solder pump is mounted to connect to other wafers. On the top side, an aluminium layer (shown in blue) forms a second empty cylinder, which overlaps with the inside, upper part of the tungsten cylinder wall. The upper side of the aluminium connects to the planar interconnect structure

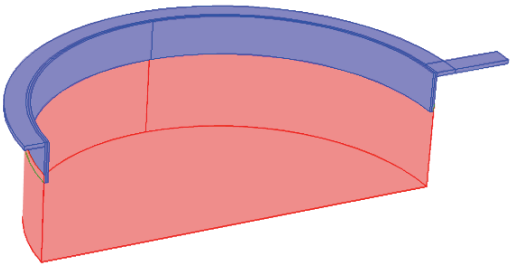

Fig. 1. TSV structure: Aluminium in blue and tungsten in red. The tungsten cylinder is shortened to 10% of the real length. For the simulated TSV the upper plate is missing.

by a round plate as shown in Fig. 1. These open (empty) TSVs are different compared to the traditional copper TSVs which have their cylinders completely filled.

Electromigration addresses the material transport due to microscopic forces acting on mobile defects. There are two forces of importance. The first is the so called direct force, caused by the the local electric field acting on the ionic atoms in the metal. The second is called the wind force, caused by the electrons scattered by the atoms in the metal [2]. Both forces together are modelled by

$$\vec{F} = \vec{F}_{direct} + \vec{F}_{wind} = (Z_d + Z_w)e\vec{E} = Z^* e\vec{E} \qquad (1)$$

were Z^* is called the effective valence, which shows the sensitivity to electromigration.

For the macroscopic modeling of the time evolution of the vacancy distribution C_v in a bulk material, a drift-diffusion model [3] with an additional generation/annihilation term G is used as:

$$\frac{\partial C_v}{\partial t} = -\nabla \cdot \vec{J}_v + G \qquad (2)$$

The generation/annihilation term G usually called Rosenberg-Ohring term [4], [5] is computed by (3) where $C_{v,eq}$ is the equilibrium concentration and τ is the characteristic relaxation time constant of the vacancy concentration.

$$G = \frac{C_{v,eq} - C_v}{\tau} \qquad (3)$$

The vacancy flux $\vec{J}_v$ is driven by four driving forces, three of which are included in the bracket of the following equation:

$$\vec{J}_v = -D_v \left(\nabla C_v - \frac{|Z^*|}{k_\mathrm{B}T} C_v \nabla \vec{E} + \frac{f\Omega}{k_\mathrm{B}T} C_v \nabla \sigma \right) \qquad (4)$$

978-1-4673-5736-4/13/$31.00 ©2013 IEEE

where $k_{\mathrm{B}}T$ has the usual meaning, D_v is the diffusion constant, Ω the atomic volume and f the relaxation factor. The first term is a typical diffusion flux term. The second flux term is caused by the electromigration as described above. The third term is the flux caused due to different stresses in the material. A fourth flux term can be due to temperature gradients in the material, but this is neglected in this study.

For the stress term a solid mechanics simulation is needed. The initial strain, which serves as an input to the solid mechanics simulation, can be obtained by the following equation [6].

$$\frac{\partial \epsilon^v}{\partial t} = -\Omega[(1-f)\,\nabla \cdot \vec{J}_v + fG] \tag{5}$$

Regarding the vacancy flow through and around the aluminium/tungsten interface, three effects have to be considered. First, the interface can partially block vacancies from passing from one metal to the other. Second, the interface can represent a sink or source of vacancies. Third, it can act as a fast diffusion path transporting vacancies parallel to it. The first effect is described by the segregation model proposed in [7] as:

$$J_{1,2} = h\,(C_2 - C_1) \tag{6}$$

$J_{1,2}$ is the vacancy flow through the interface and h the transport coefficient. $h = 0$ means a fully blocking interface. The second effect is modelled as a lower equilibrium concentration for the interface. This interface behaviour can be easily implemented by including a finite thickness for the interface in the simulation domain. This finite domain includes part of the aluminium region, the interface, and part of the tungsten region. The bulk equation (2) is then solved for this interface domain. The third effect is modeled by using a higher diffusion coefficient D_v in the interface region for (4), also employing the finite thickness interface domain approximation described above.

Two series of model parameter variations were carried out using FEDOS, an in-house Finite-Element-Method (FEM) program, containing all known EM models [3]. The first series is a variation of the vacancy conductivity. The second a variation of the sink behaviour (the parameter $C_{v,eq}$ in (3) hereafter referred to as C_{inter} to make it distinguishable to the bulk value). The schematic structure depicted in Fig. 2 is used. Out of these simulations the worst EM case (highest vacancy concentration at the interface) is estimated. These worst case parameters are then used to simulate the stress built-up and vacancy flow in the structure shown in Fig. 1. The mechanical constraints were chosen as follows: The outside of the cylinder is surrounded by silicon oxide substrate. Therefore, the position of the outer surface of the material is considered to be fixed. Inside the cylinder there is a thin silicon oxide layer which allows the inner aluminium surface to move, so the free boundary condition is employed.

III. Results

First, finite element simulations were carried out to find the locations with the highest current densities in order to estimate,

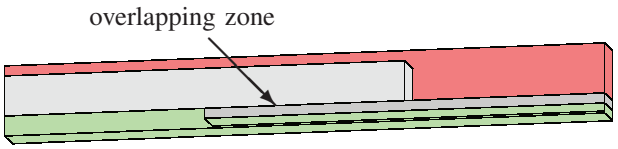

Fig. 2. Simplified structure of the aluminium/tungsten interface for the interface simulation. Aluminium in bright grey and tungsten in dark grey. Red and green the surrounding silicon oxide and titanium nitride layers.

Fig. 3. Current density in the upper TSV structure near the feeding interconnection with high current densities in red and low in green regions.

where electromigration will have the highest influence. The result is depicted in Fig. 3, where the red coloured regions carry high current densities and the green regions carry low current densities. Regions with the highest current are located at the overlapping zone under the current carrying interconnect on the right side of the figure. In that region (the right vertical edge of Fig. 3), the aluminium and tungsten connect as indicated in Fig. 2 above. This justifies why the structure shown in Fig. 2 is chosen to investigate the impact of the different interface behaviours. Here, the curvature of the cylinder is neglected. This approximation is justified as the aluminium and especially the tungsten thickness is small compared to the radius of the cylinder.

Fig. 4 shows the current density distribution and direction from the EM simulation at the interface between the tungsten and the aluminium in the structure of Fig. 2. The upper line represents the aluminium and the lower line the tungsten. The current density distribution of the EM simulation shows that at the interface two kinds of regions can be distinguished. In the middle region of the overlapping zone of the aluminium/tungsten interface, the current density flows parallel to the interface in the z-direction. At the very beginning and end of the overlapping region, on the other hand, the current density direction has a high component orthogonal to the interface and to the z-direction as shown by the cones. As will be shown below, this orthogonal flow strongly affects the vacancy concentration near the interface.

Fig. 5 shows the vacancy concentration around the interface, normalised to the bulk aluminium or tungsten vacancy concentration (assumed to be the same) along the interface (z-direction). The two vertical lines indicate the overlapping zone of the two materials. The vacancy density lines of

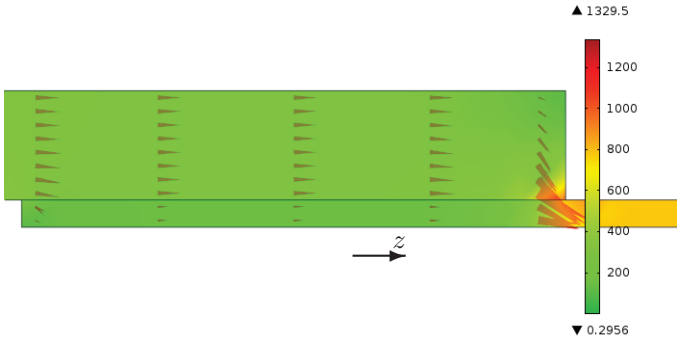

Fig. 4. Current density (in kA/cm^2) in the simulated structure. Cones are showing the direction of the current density. Upper part is aluminium and lower part is tungsten.

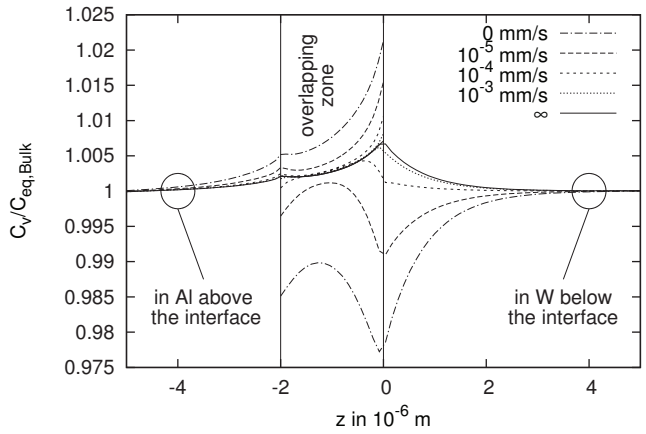

Fig. 5. Segregation model: Variation of the transport coefficient. Vacancy density in aluminium and in tungsten versus the location of the interface.

aluminium end at the right border of the overlapping zone as also the aluminium does. Similarly, the vacancy density lines of tungsten end up on the left border. From this figure, one can see that the highest vacancy concentration differences between the two metals, arise in the regions through which the highest current density orthogonal to the interface occurs (in the right side of the overlapping zone, around z=0). At the left side of the interface, a smaller peak also appears due to the higher orthogonal current density component as seen in Fig. 4. In these two regions, a large concentration of vacancies reaches the interface and piles up there. Whether the vacancies are able to transfer to the opposite region, depends on the vacancy conductivity (h) in (5). Fig. 5 shows the vacancy concentration using several possible values of h, varying from 0 mm/s to 10^{-3} mm/s. Indeed, as the h parameter increases, the vacancies can more easily flow through the interface, and the concentration which is blocked around the interface is reduced.

Fig. 6 shows the time evolution of the vacancy concentration for a highly blocking interface ($h = 10^{-5}$ mm/s) in arbitrary time units. A steady state for the vacancy concentration is

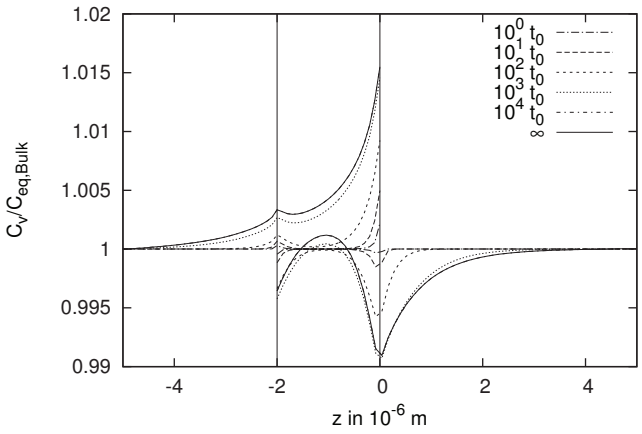

Fig. 6. Segregation model: Simulation of a highly blocking interface ($h = 10^{-5}$ mm/s) for different time steps in arbitrary t_0 units.

reached after approximately $t = 10^4\, t_0$. In this steady state, the electromigration flux is in equilibrium with the vacancy diffusion flux and the generation/annihilation term.

Next, the results of the variation of the equilibrium concentration for the Rosenberg-Ohring term in the interface ($C_{v,eq}$ in (3)) are depicted in Fig. 7. Again, all concentrations are normalised by the bulk aluminium/tungsten equilibrium concentration. It should be noted that in this calculation the interface boundary is fully open, i.g. $h = \infty$. The minimum vacancy concentration is observed in the middle of the interface, as no orthogonal component of the current density is transporting vacancies there. At the left/right sides of the interface, the non-zero orthogonal component of the current is flooding the interface with vacancies. Fig. 8 shows the time evolution for the highest sink strength, $C_{inter} = 0$.

According to the results above, the highest vacancy concentration around the interface is reached: i) when the interface acts as a fully blocking barrier, ii) when the interface shows no sink behaviour, i.g. the same equilibrium concentration as in the surrounding bulk material is available (as expected). Therefore, the analysis further on considers these interface conditions as the worst case scenario. These simulations are performed for the TSV structure of Fig. 1 in order to examine how the built-up stress in the structure will look like. The stress profile at the inner cylinder surface is shown in Fig. 9, whereas the profile at the outside surface is shown in Fig. 10. In these simulations, only the aluminium structure is simulated due to the blocking interface and the mechanical constraints. Furthermore the vacancy flow in tungsten is negligible due to the blocking interface assumed. The highest stress was found at the inside of the aluminium cylinder. There are two peaks of high stress, one at the beginning and an other at the end of the overlapping zone. These are, therefore, the zones where stress induced damage is most likely to occur. On the interface zone there are no stress peaks visible. In addition, on the top of the aluminium cylinder there is no stress at all. This also justifies neglecting the upper aluminium plate in the simulations of the

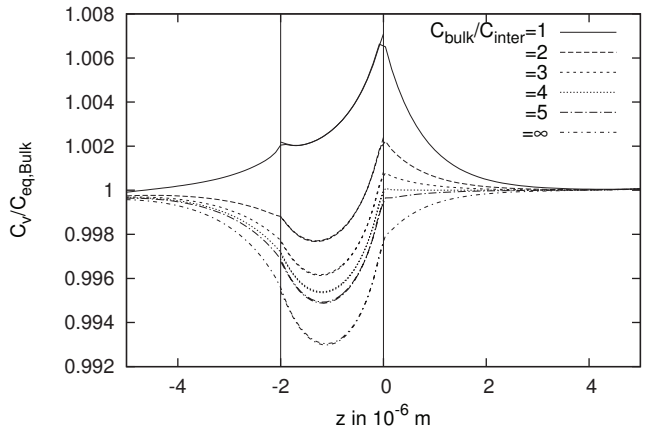

Fig. 7. Rosenberg-Ohring model: Variation of the equilibrium concentration in the interface region.

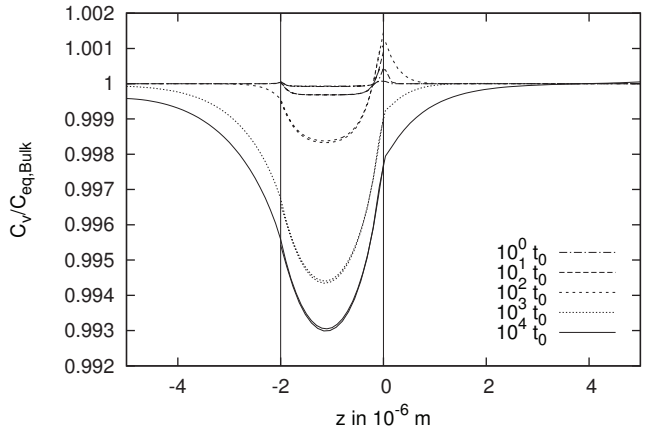

Fig. 8. Rosenberg-Ohring model: Result at different time steps for the lowest possible equilibrium concentration ($C_{inter} = 0$).

real structure (Fig. 1).

All results show a localised EM influence, extending only approximately a few μm around the interface region. Therefore the EM studies can be restricted to these critical parts of the structures and can then be used as an overall predictor of the resistance against EM degradation of the entire structure.

IV. Conclusions

In this work the impact of the interface behaviour between tungsten and aluminium regarding electromigration in open TSVs is studied. The worst case values for the segregation model and the Rosenberg-Ohring term of the interface, with respect to the vacancy concentration have been identified. The segregation model predicts the highest concentrations, when the vacancy transport is fully blocked between the two metals and the Rosenberg-Ohring term is not acting as a sink. This kind of interface characteristic was then used for the electromigration and the stress calculation in a TSV structure. These simulations showed that the highest stress is close to the

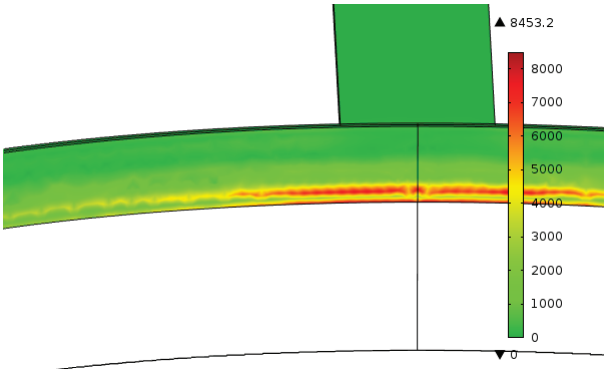

Fig. 9. Von Mises stress (in N/cm^2) on the inner surface of the aluminium cylinder.

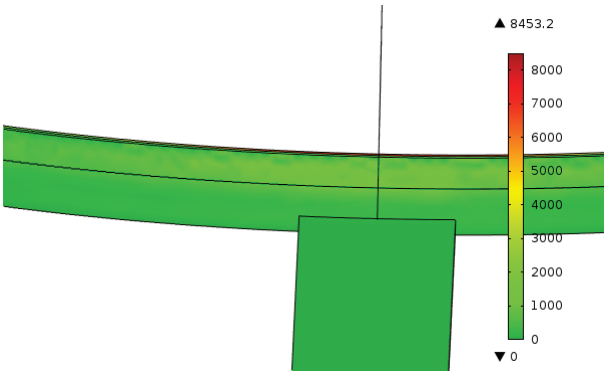

Fig. 10. Von Mises stress (in N/cm^2) on the outer surface of the aluminium cylinder.

interface at the inner surface of the aluminium cylinder near the interconnect of the structure. Surprisingly, only limited stress has been observed at the interface of the two materials and at the outer surface of the TSV. These results regarding the stress build up due to electromigration show the sites where stress induced degradation will most probably occur.

References

[1] J. Kraft, F. Schrank, J. Teva, J. Siegert, G. Koppitsch, C. Cassidy, E. Wachmann, F. Altmann, S. Brand, C. Schmidt, and M. Petzold, "3D sensor application with open through silicon via technology," *Electronic Components and Technology Conference*, pp. 560–566, 2011.

[2] R. S. Sorbello, "Microscopic driving forces for electromigration," *Proc. Mater. Research Soc. Symp.*, vol. 427, pp. 73–81, 1996.

[3] R. L. de Orio, "Electromigration modeling and simulation," Ph.D. dissertation, Technische Universität Wien, June 2010.

[4] R. Rosenberg and M. Ohring, "Void formation and growth during electromigration in thin films," *Journal of Applied Physics*, vol. 42, no. 13, pp. 5671–5679, 1971.

[5] H. Ceric, R. De Orio, J. Cervenka, and S. Selberherr, "A comprehensive TCAD approach for assessing electromigration reliability of modern interconnects," *Device and Materials Reliability, IEEE Transactions on*, vol. 9, no. 1, pp. 9–19, 2009.

[6] H. Ceric, R. Heinzl, C. Hollauer, T. Grasser, and S. Selberherr, "Microstructure and stress aspects of electromigration modeling," *AIP Conference Proceedings*, vol. 817, no. 1, pp. 262–268, 2006.

[7] F. Lau, L. Mader, C. Mazure, C. Werner, and M. Orlowski, "A model for phosphorus segregation at the silicon-silicon dioxide interface," *Applied Physics A*, vol. 49, no. 6, pp. 671–675, 1989.